

Rotating single atoms in a ring lattice generated by a spatial light modulator

Xiaodong He^{1,2,3}, Peng Xu^{1,2,3}, Jin Wang^{1,2}, and Mingsheng Zhan^{1,2,*}

1 State Key Laboratory of Magnetic and Atomic and Molecular Physics, Wuhan Institute of Physics and Mathematics, Chinese Academy of Sciences - Wuhan National Laboratory for Optoelectronics, Wuhan 430071, China

2 Center for Cold Atom Physics, Chinese Academy of Sciences, Wuhan 430071, China

3 Graduate University of the Chinese Academy of Sciences, Beijing 100049, China

*mszhan@wipm.ac.cn

Abstract: We demonstrated trapping single neutral Rb atoms in micro traps of an optical ring lattice formed by superposing the $\pm l$ components of the Laguerre-Gaussian mode, and generated by reflecting a single laser beam from a computer controlled spatial light modulator. A single atom in one trap or two atoms with one each in two traps were identified by observing the fluorescence. The trap array loaded with single atoms was rotated by dynamically displaying the hologram animation movie on the modulator. The modulation period in the fluorescence indicates the rotation of one or two single atoms in the lattice.

© 2009 Optical Society of America

OCIS codes: (020.3320) Laser cooling; (020.7010) Laser trapping; (270.5585) Quantum information and processing; (090.2890) Holographic optical elements.

References and links

1. R. Grimm, M. Weidemüller, Y. B. Ovchinnikov, "Optical dipole traps for neutral atoms," *Adv. At., Mol., Opt. Phys.* **42**, 95-170 (2000).
2. D. Frese, B. Uberholz, S. Kuhr, W. Alt, D. Schrader, V. Gomer, and D. Meschede, "Single atoms in an optical dipole trap: Towards a deterministic source of cold atoms," *Phys. Rev. Lett.* **85**, 3777-3740 (2000).
3. N. Schlosser, G. Reymond, I. Protchenko, P. Grangier, "Sub-poissonian loading of single atoms in a microscopic dipole trap," *Nature (London)* **411**, 1024-1027 (2001).
4. S. Bergamini, B. Darquie, M. Jones, L. Jacubowicz, A. Browaeys, P. Grangier, "Holographic generation of microtrap arrays for single atoms by use of a programmable phase modulator," *J. Opt. Soc. Am. B* **21**, 1889-1894 (2004).
5. R. Dumke, M. Volk, T. Muther, F.B.J. Buchkremer, G. Birkl, W. Ertmer, "Micro-optical Realization of Arrays of Selectively Addressable Dipole Traps: A Scalable Configuration for Quantum Computation with Atomic Qubits," *Phys. Rev. Lett.* **89**, 097903 (2002).
6. D. Schrader, I. Dotsenko, M. Khudaverdyan, Y. Miroshnychenko, A. Rauschenbeutel, and D. Meschede, "Neutral Atom Quantum Register," *Phys. Rev. Lett.* **93**, 150501 (2004).
7. Y. Miroshnychenko, W. Alt, I. Dotsenko, L. Forster, M. Khudaverdyan, D. Meschede, D. Schrader, A. Rauschenbeutel, "Quantum engineering: An atom-sorting machine," *Nature (London)* **442**, 151 (2006).
8. S. Kuhr, W. Alt, D. Schrader, I. Dotsenko, Y. Miroshnychenko, W. Rosenfeld, M. Khudaverdyan, V. Gomer, A. Rauschenbeutel, D. Meschede, "Coherence properties and quantum state transportation in an optical conveyor belt," *Phys. Rev. Lett.* **91**, 213002 (2003).
9. O. Mandel, M. Greiner, A. Widera, T. Rom, T.W. Hansch, I. Bloch, "Coherent transport of neutral atoms in spin-dependent optical lattice potentials," *Phys. Rev. Lett.* **91**, 010407 (2003).
10. J. Beugnon, C. Tuchendler, H. Marion, A. Gaetan, Y. Miroshnychenko, Y.R.P. Sortais, A.M. Lance, M.P.A. Jones, G. Messin, A. Browaeys, P. Grangier, "Two-dimensional transport and transfer of a single atomic qubit in optical tweezers," *Nat. Phys.* **3**, 696-699 (2007).
11. S. Franke-Arnold, J. Leach, M.J. Padgett, V.E. Lembessis, D. Ellinas, A.J. Wright, J.M. Girkin, P. Ohberg, A.S. Arnold, "Optical ferris wheel for ultracold atoms," *Opt. Express* **15**, 8619-8625 (2007).

12. L. Allen, M. W. Beijersbergen, R.J.C. Spreeuw, and J. P. Woerdman, "Orbital angular momentum of light and the transformation of Laguerre-Gaussian laser modes," *Phys. Rev. A* **45**, 8185 - 8189 (1992).
13. T. Kuga, Y. Torii, N. Shiokawa, T. Hirano, Y. Shimizu, H. Sasada, "Novel Optical Trap of Atoms with a Doughnut Beam," *Phys. Rev. Lett.* **78**, 4713 - 4716 (1997).
14. M. Stutz, S. Groblacher, T. Jennewein, A. Zeilinger, "How to create and detect N-dimensional entangled photons with an active phase hologram," *Appl. Phys. Lett.* **90**, 261114 (2007).
15. J. Wang, L. Zhou, R.B. Li, M. Liu, M.S. Zhan, "Cold atom interferometers and their applications in precision measurements," *Front. Phys. China* **4**, 179-189 (2009).
16. K. Li, L. Deng, E.W. Hagley, M.G. Payne, and M.S. Zhan, "Matter-wave self-imaging by atomic center-of-mass motion induced interference," *Phys. Rev. Lett.* **101**, 250401 (2008).
17. N. Schlosser, G. Reymond, and P. Grangier, "Collisional Blockade in Microscopic Optical Dipole Traps," *Phys. Rev. Lett.* **89**, 023005 (2002).
18. H. Hanbury-Brown and R.Q. Twiss, "Correlation between photons in two coherent beams of light," *Nature (London)* **177**, 27-29 (1956).
19. M. Weber, J. Volz, K. Saucke, C. Kurtsiefer, H. Weinfurter, "Analysis of a single-atom dipole trap," *Phys. Rev. A* **73**, 043406 (2006).
20. M.P.A. Jones, J. Beugnon, A. Gaetan, J. Zhang, G. Messin, A. Browaeys, and P. Grangier, "Fast quantum state control of a single trapped neutral atom," *Phys. Rev. A* **75**, 040301(R) (2007).
21. A. Browaeys, H. Häffner, C. McKenzie, S. L. Rolston, K. Helmerson, W.D. Phillips, "Transport of atoms in a quantum conveyor belt," *Phys. Rev. A* **72**, 053605 (2006).

1. Introduction

Optical dipole traps for neutral atoms rely on the electric dipole interaction between the atoms and a far-detuned light. A mK range of trap depths is enough for precooled atomic ensembles with temperature of μK range. In the traps the optical excitation can be kept extremely low. Under appropriate conditions, the trapping mechanism is independent of the particular magnetic sub-level of the electronic ground state[1]and the atomic coherence times up to several seconds are possible[2]. Meanwhile, by using light modulation techniques, microscopic optical dipole traps[3] for single atoms have been experimentally demonstrated. Because of their good scalability and long coherence time, these micro traps offer a promising way for manipulating both internal and external degrees of freedom of atoms, thus make it possible for neutral atoms to be one of the most promising candidates for storing and processing quantum information.

To store quantum information, dipole trap arrays have to be addressable to each individual trap. These traps have been demonstrated based on holographic generation by use of a spatial light modulator(SLM)[4], micro-fabricated arrays of diffractive or refractive lenses[5],or active rearrangement of single atoms by optical lattice[6] [7]. On the other hands, to process quantum information, i.e to carry out quantum computation, a gate operation between two arbitrary qubits of the register is essential. Along this way, transportation of a neutral-atom qubit has been demonstrated using 'optical conveyor belts'[7] [8],state-dependent moving optical lattices[9],and two dimensional moving tweezers[10] etc..

The above mentioned holographic optical traps implemented by a computer controlled SLM uses a single collimated beam. The SLM transforms the single Gaussian beam into arbitrary intensity patterns which are then focused by a high numerical aperture lens onto an array of traps (i.e. optical lattice). The advantage of these systems is that the holograms corresponding to various arrays of traps can be designed, calculated, and optimized on a computer. The lattice can be controlled and reconfigured by writing these holograms on the SLM in real time.

Here, we employ a computer controlled SLM to construct ring lattice which was proposed and demonstrated in [11]. Instead of superposing a pair of separated Laguerre-Gaussian (LG) beams with l and $-l$ indices, we obtain the ring lattice by imposing the phase of the superposed Laguerre-Gaussian modes($\pm l$) directly to the SLM and focusing a single laser beam onto the SLM. We trap and address single rubidium(^{87}Rb) atoms in the individual traps of the ring lattice. Under rotation symmetry conditions of the holograms that generate the ring lattice, we two-dimensionally transport single atoms by imposing a series of holograms onto SLM with

video resolution and refresh rates.

2. The ring lattice and its hologram generation

As we know, Laguerre-Gaussian(LG_p^l) beams possess orbital angular momentum along the optical axis when l is not zero, where p and l are the radial and azimuthal indices of the LG modes[12]. Among them, the $p=0$ modes $LG_{p=0}^l$, called doughnut beam, have a spiral phase structure, hence the phase is undefined on the optical axis where light intensity must be zero[13]. The complex scalar function describing the distribution of the field amplitude of a $LG_{p=0}^l$ beam using a laser power P at wavelength λ can be expressed cylindrically as [11][12]:

$$LG_{p=0}^l = \sqrt{I} \sqrt{\frac{2}{\pi |l|!}} \left(\sqrt{2}r/w \right)^l \exp(-r^2/w^2) \exp\left(-i \frac{kr^2z}{2(z^2 + z_R^2)}\right) \exp(-il\phi) \exp\left(i \left((l+1) \tan^{-1} \frac{z}{z_R} \right)\right),$$

where $I = Pw^{-2}$ is the laser intensity, $z_R = \pi w_0^2/\lambda$ is the Rayleigh range, and $w = w_0 \sqrt{1 + (z/z_R)^2}$ is the beam waist. By interfering co-propagating two LG beams with opposite azimuthal indices l we obtain a ring lattice intensity distribution, which comprises $2l$ petals[11]:

$$I_{ring} = \left| LG_{p=0}^l + LG_{p=0}^{-l} \right|^2 = I \frac{2}{\pi |l|!} \left(\sqrt{2}r/w \right)^{2|l|} \exp(-2r^2/w^2) (2 + 2\cos(2l\phi)).$$

Experimentally, we can realize the LG beams and the ring lattice by using a SLM. Instead of interfering the two co-propagating LG beams produced by the SLM[11], in the following we directly generate the ring lattice by imposing the holograms containing the superposition of the LG beams' phase onto the SLM. In this way, since the ring lattice is generated from a single beam, it is insensitive to any vibration and is easier to align.

The SLM we used is a reflective liquid crystal phase modulator(Holoeye, HEO 1080P) with a resolution of 1920*1080 pixels and pixel size of $8 \times 8 \mu m^2$. The SLM works like a computer monitor at 60Hz video rate, i.e. it uses the DVI (Digital Visual Interface) monitor output of a computer graphics card as its input driver, and it just displays a copy of the image at the desktop, but it converts the graphic movie into a continuous phase pattern animation. At the desktop one can open image application software window containing the hologram pattern, which can be adjusted easily to the optical axis of incident laser under mouse-control like ordinary window on a computer monitor. The 8-bit gray value holograms depicted at the SLM are presented as 256(0-255) phase levels that control the phase change of the reflected laser. At our wavelength (830nm) programmable phase shift in a range between 0 and 2π are obtained. The total diffraction efficiency into the first order is about 40%.

In order to generate the ring lattice hologram we implemented an algorithm that has details in the reference[14] by using the MATLAB[®] software. The function generating the output hologram displayed on the SLM is

$$\text{mod}[(\text{angle}[LG(x, y, l, z, w_0, z_R) + LG(x, y, -l, z, w_0, z_R)] + x \cdot kx), 2\pi] \cdot \frac{256}{2\pi}, \quad (1)$$

where $LG(x, y, l, z, w_0, z_R)$ and $LG(x, y, -l, z, w_0, z_R)$ are the LG beams with opposite azimuthal indices l . The term $\text{angle}[LG(x, y, l, z, w_0, z_R) + LG(x, y, -l, z, w_0, z_R)]$ is the ring lattice phase pattern. The phase pattern has $2l$ symmetrical jumps of π for $l > 1$ and one phase jump of π for $l = 1$. The corresponding mode consists of $2l$ petals(see Fig. 1). And $x \cdot kx$ is a blazed

phase grating structure, acting as a tilted mirror to separate the 1st-order ring lattice from the 0th-order non-modulated light.

To observe and record the microscopic ring lattice, we image the light onto a CCD camera after magnification by a factor of 50 by an aberration-free objective group. Figure 1 shows the CCD images of the ring lattices of $l = [1, 2, 3]$ and the corresponding holograms calculated by Eq. (1).

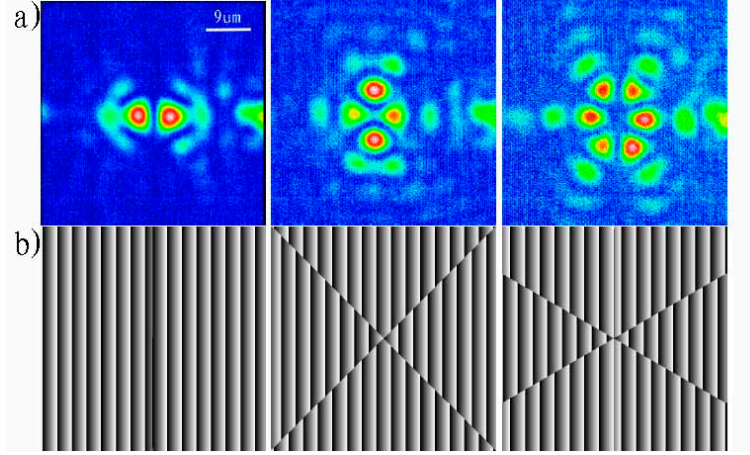


Fig. 1. (color online) The ring lattices of $l = [1, 2, 3]$ and their holograms. Observed optical intensity distribution of the ring lattices(a) and the corresponding gray-level holograms with 600×600 pixels(b).

3. Dynamically rotating the ring lattice

As described above, the laser has a phase pattern with $2l$ symmetrical jumps of π for $l > 1$ and one phase jump of π for $l = 1$, the corresponding intensity pattern consists of $2l$ petals. If we change the azimuthal positions of jumps of π , we can then change the azimuthal position of the intensity maxima. To achieve this, we can add an offset φ to the azimuthal angle ϕ . To obtain maximum rotation rate and preserve the periodicity of the rotation progress, we set the offset step φ to $\frac{2\pi}{N}$, with N satisfying $\text{mod}(60, N) = 0$, i.e.

$$\text{mod}[\text{angle}[LG(x, y, l, z, w_0, z_R) \cdot \exp(il(J-1)\varphi) + LG(x, y, -l, z, w_0, z_R) \cdot \exp(-il(J-1)\varphi)] + x \cdot kx, 2\pi] \cdot \frac{256}{2\pi}.$$

The rotation rates of the whole ring lattice are equal to $60/N$ Hz. From geometrical symmetry, we can learn that values of $N=1, 2$ correspond to adding 2π and π step to the original azimuthal positions, which does not change the shape of the ring lattice. Thus the maximum rotation rate we can obtain is 20Hz ($N=3$) in our scheme.

To generate rotating holograms, we calculated a series of different values of J (1 to 60), and converted the output holograms to an AVI version's video with maximum frames per second (fps) of 60. The video lasts for 1 second. When playing the hologram movie on the desktop, the rotating holograms were displayed on the SLM with video resolution and the same refresh rates, thus the ring lattices rotated. Figure 2 shows the optical signals of the rotating $l = \pm 1$ ring lattice at different rotation rates detected by a photodetector (New Focus, Model 1621). The signals were recorded by a digital storage oscilloscope (Tektronix, TDS2014B) and the sample

interval is 1ms. The signals suggest that the ring lattices are rotating smoothly in real time. The peak heights are not the same, meaning that the light intensities of the two traps are not equal.

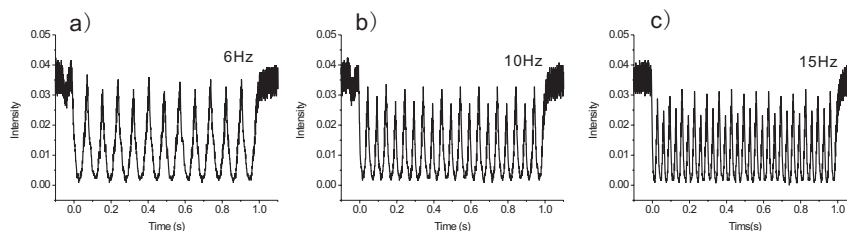


Fig. 2. The optical signals of rotating ring lattice ($l = \pm 1$, two traps) for different rotation rates $60/N$ Hz with $N=10$ (a), 6(b) and 4(c). The rotation lasts for 1 sec.

4. Trapping single atoms in the ring lattice and rotating the single atoms

With the ring lattice we now demonstrate the ability of trapping and rotating single atoms. For this purpose we used a lattice with two traps which was generated by hologram of $l = \pm 1$. A typical laser power of 10mW was assigned to each trap. This laser intensity corresponds to an optical potential depth of 1mk for ^{87}Rb atoms. The experimental setup is shown in Fig. 3. We started with a standard $\sigma^+ - \sigma^-$ 6-beam retro-reflected magnetic-optical trap (MOT) that is loaded from a background rubidium vapor in an ultrahigh vacuum[15][16]. Each MOT beam has an intensity of $14\text{mW}/\text{cm}^2$ and is 12MHz red-detuned from the $F = 2 \rightarrow F' = 3$ cycling transition at 780nm. A repumping beam tuned to the $F = 1 \rightarrow F' = 2$ transition is superimposed with the MOT beams. These beams are directed onto the center of the magnetic quadrupole field which is produced by two magnetic coils in anti-Helmholtz configuration. The coils can generate magnetic field gradients of up to 10G/cm at a current of 1.4 A. The typical temperature of the cold atom cloud in the MOT is on the order of $100\mu\text{K}$. Then we focused the ring lattice to a waist of $2.5\mu\text{m}$ by using a microscopic objective lens with $\text{NA}=0.38$. The ring lattice is loaded by simply overlapping it with the cold atom cloud in the MOT. By adjusting the MOT parameters (reducing the intensity and increasing the detuning), we could decrease the density of the cloud, and enter the regime where the loading rate of atom is less than 1s^{-1} for each trap. The MOT light induced fluorescence (LIF) of atoms in the optical trap region was collected with the same microscopic objective lens, and separated from trapping beam with a dichroic mirror. Then the LIF was coupled into a single mode fiber (with diameter $10\mu\text{m}$) at 1550nm wavelength for spatial filtering with magnification by a factor 1 and detected with an avalanche photodiode (APD) assembled in a single photon counting mode (SPCM, EG&G AQRH-14-FC). Because of the moderate diameter of the fiber for the size of double traps, we can selectively collect the LIF from the double traps simultaneously or any one of trap individually by adjusting the kinematical mounts of our image system. We used an interference filter (centered at 786 nm, with 26 nm bandwidth) to block the stray light of the dipole trap laser.

Figure 4(a) shows a time sequence of the LIF signal observed in 20ms time bins. To get this figure, we focused the imaging system onto an individual trap of the lattice. The sudden jumps in the fluorescence signal correspond to a single atom entering the trap and being trapped, while the sudden drops result from atom leaving the trap due to a collision with another incident atom. The process of two atoms being ejected from the trap occurs because of light-assisted collision by the MOT lasers at 780 nm. Pairs of atoms were hardly observed in a trap, which indicates that the waist of the optical trapping beam is no more than a few microns, so that the loss rate due to two-body collisions becomes huge and the condition of "collisional blockade

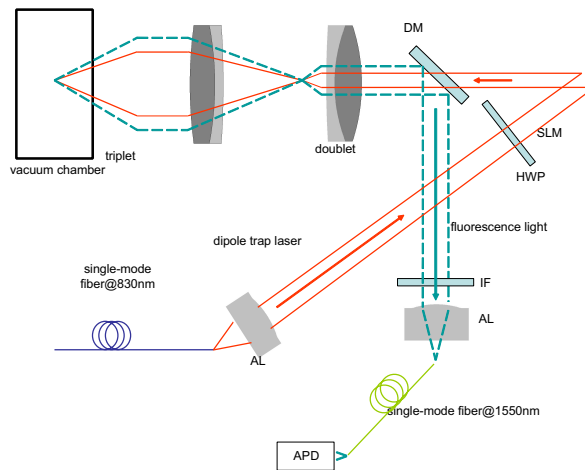


Fig. 3. Experimental setup for trapping and rotating single atoms. Both optical ring lattice (solid line) and optical imaging (dotted line) systems are shown (not to scale). The incident linearly polarized light from a single mode laser diode at 830nm is delivered and collimated by a single mode polarization maintaining fiber with an output NA=0.11 and an aspherical lens(AL). A half-wave plate(HWP) rotates the light polarization axis to match the polarization required by the SLM. The laser is then reflected by the SLM and expanded by two doublets and focused onto the MOT region by a triplet. The triplet is also used as an imaging system to collect the fluorescence at 780nm of the atoms. The fluorescence is separated from the dipole laser by a dichroic mirror(DM) and is passed through an interference filter(IF) before entering the spatial filter of a single mode fiber at 1550nm.

mechanism”[3] [17] is satisfied. We have also made the HBT (Hanbury Brown and Twiss effect) measurement[18](see Fig. 4(b)), the result shows that the fluorescence does come from a single atom [19]. In Fig. 4(c) we then focused the imaging system onto whole ring lattice, and the progress of two atoms with one loaded in each trap was monitored. The secondary jumps in the figure indicate that two atoms are indeed trapped simultaneously for some times in the ring lattice. The loading progress of a single atom is completely stochastic and independent, so the probability of detecting two single atoms being in the double traps is smaller than detecting single atom in the individual trap[4].

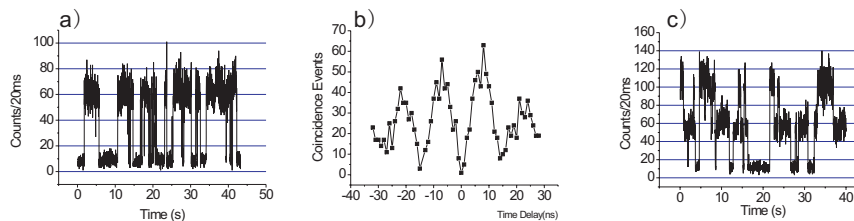


Fig. 4. Fluorescence of single atoms measured by SPCM. Each point corresponds to a 20 ms time bin. Shown in (a) is the fluorescence signal from atom in an individual trap. (b) is the measurement of second-order correlation function $g^{(2)}(\tau)$ of single atom fluorescence. (c) is the fluorescence signal from the whole two traps in the ring lattice.

To rotate single atoms in the ring lattice and monitor the rotating progress, we first realigned the imaging system and limited our observation view field only to one trap as in Fig. 4(a). Once the photon counting rate exceeded a threshold value thus indicating that an atom was trapped, the MOT and repumping beam was switched off for 40ms to let the atoms trapped in the MOT diffuse out of the ring lattice region. Then the MOT beams and the repumping beam were turned on to detect the single atoms, the hologram video was played on the SLM and the lattice with one atom in it was forced to rotate. The LIF was continuously recorded during the rotating process. Because of the limited view field of the image system, when the atom is rotated out of the field, the counting rate would decrease until the atom is moving back. The fluorescence signal of the single rotating atom should display an oscillation with frequency equal to the rotation rate of the holograms(15Hz), as shown in Fig. 5(a). Under this condition, if the ring lattice with two atoms in the two traps (one each), the collection system would get twice maximum counting rate in one period, so fluorescence signal should display an oscillation with frequency (12Hz) twice the rotation rate (6Hz), as shown in Fig. 5(b). To ensure that the single atom is really rotating with the lattice, we built another image system to detect the LIF from north pole position of the ring where no trapped atom at the beginning (see the leftmost picture of Fig. 1(a)). When the single atom rotates with ring lattice and passes by the north pole point, this collection system should also see the oscillating LIF with some time delay. Shown in Fig. 5(c) is the fluorescence signals recorded by aiming at the left trap (solid line) where the atom is initially trapped, and at the upper north-pole (dashed line). Since the ring lattice was clockwise rotating, the upper pole signal is about 1/4 period late than the left trap signal.

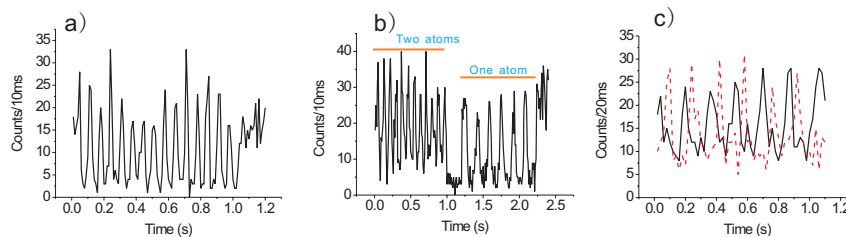


Fig. 5. The modulated fluorescence signal of single atoms rotated in the ring lattice. (a) The rotation rate is 15 Hz, viewed to a single atom in a trap; (b) The rotation rate is 6 Hz. In the first second, two atoms are trapped which give fluorescence of 12Hz; in the second second, an atom is lost, thus the remaining atom produces a signal of 6 Hz. (c) Single atom signals recorded at the left trap (solid line) and the upper north-pole (dashed line). The rotation rate of the lattice is 6Hz.

5. Conclusion

We have experimentally demonstrated trapping and rotating single atoms in a ring lattice generated by a computer controlled spatial light modulator. For the first time we rotated the single atoms in the ring lattice by use of SLM with video refresh rate. This opens up possibilities for constructing quantum register: qubits can be encoded in the hyperfine levels of ground state of the single atoms in different traps. The initial state preparation and single-qubit operations can be achieved with Raman pulses. As demonstrated in [20], dipole trap laser can serve as one of the Raman pulse. We can send another Raman beam to the rotation region and to transfer the atoms. This step will accomplish a single qubit manipulation. Furthermore we could simultaneously rotate the atomic qubits in the ring lattice, by coupling and modulating the Raman beam into the same fiber as dipole traps. The ability of dynamically manipulating single atoms in the trap-arrays by SLM also opens door for testing schemes for atom-atom entanglement

recommended in reference [4]. Technically, limited by the slow video refresh rate, at present the rotation rate of the ring lattice for single atom is only 15 Hz. To overcome this limitation, a versatile optical ring lattice with a tunable rotation rate from a few mHz to 100's MHz [11] can be used. The ring lattice could be rotated smoothly and continuously in much faster speed compared to our scheme. But for adiabatically transporting single atom qubit in the trap, the acceleration a of the rotating trap must fulfill $ma\sigma \ll \hbar\Omega$ (where Ω is the oscillation frequency of the atom, m its mass and σ the extension of the ground state wave function)[10][21]. For our experimental parameters, kHz rotation rate for atoms could be obtained with this method.

Acknowledgements

This work was supported by the National Basic Research Program of China under Grant No.2006CB921203, by the National Natural Science Foundation of China under Grant Nos.10827404 and 10804124, and also by funds from the Chinese Academy of Sciences.